Frequency-Domain Methods in Optical Tomography: Detection of Localized Absorbers and a Backscattering Reconstruction Scheme

John S. Maier and Enrico Gratton

Laboratory for Fluorescence Dynamics, Department of Physics,
University of Illinois at Urbana-Champaign, 1110 West Green Street,
Urbana, IL 61801-3080

ABSTRACT

We studied the ability to detect small absorbing objects embedded in a highly scattering medium. Absorbing spheres of varying size, from 0.8 mm to 6.8 mm radius, submerged in a solution of highly scattering, low absorbing liquid: skim milk, were studied in a trans-illumination geometry. Groups of more than one sphere and a single circular disk, with radius identical to that of one of the spheres, were also studied. Single linear raster scans in the plane of the sphere, with the spheres centered between the source and detector, were made. Data was taken in the frequency-domain, yielding profiles of the objects in each of the three measurable quantities: DC intensity, phase, and modulation. The diffraction pattern from the sphere differed from that of the disk, demonstrating a volume effect associated with photon diffusion. The diffraction pattern of multiple spheres differed from that of single spheres. We have also performed a frequency-domain study of the bundle of trajectories from the source to the detector when both are on the surface of a highly scattering material in the so-called "back-scattering" geometry. With a 7.2 cm source detector separation the bundle of photons that travel from the source to the detector is fairly well localized. The good localization and deep penetration are characteristics which form the basis for a three-dimensional (3-D) image reconstruction method. Using a model bundle and backscattering measurements taken at the surface, one can construct a 3-D histogram of the photon density below the surface. Since the photon density depends on the local absorption and scattering coefficients, a reconstruction of spectroscopic maps of these parameters might be possible. The AC bundle is sharpest at high frequencies while its depth of penetration seems independent of the modulation frequency. The highest useful frequency is determined by the signal-to-noise ratio of the system.

1. INTRODUCTION

Because of the high scattering to absorption ($\mu s/\mu a$) ratio for near-infrared light in human tissues, its behavior in them can be modeled by diffusion. Each diffusing photon travels a random walk path and, therefore, samples much more volume than a straight path through the tissue. Because of this, the diffusing photons carry more information about embedded structures than the straight line photons. The straight line photons sample only the cross section of the embedded object, while the diffusive photons carry information about its 3-D structure. Also, due to the volume sampling random walk of the diffusive photons, the information carried in diffusive photons is averaged over a large volume, and information about small, local inhomogeneities is difficult to obtain. The feasibility of using near-infrared light to do imaging of human tissues depends on how easy it is to detect objects embedded in tissues. The use of near-infrared to diagnose

0-8194-1115-9/93/$6.00

breast cancer, for example, depends on the ability to detect groups of millimeter-sized tumor precursors against the background of the breast.

Finally, because each individual photon undergoes a random walk, it is impossible to calculate each photon's path. One can, however, determine their average path. This is a particularly interesting question concerning the so-called "backscattering geometry," where both the source and detector are placed on the surface of a highly scattering material. The photons that travel from the source to the detector tend to follow a banana-shaped path that extends below the surface[1]. Time-resolved backscattering measurements, combined with information about the localized bundle of photon trajectories from the source to the detector, should allow one to construct a 3-D map of the scattering and absorption coefficients below the surface. As in MRI and X-Ray, a map of these physical properties could provide anatomical information. In addition, because of the sensitivity of the absorption coefficient to local physiological activity (i.e., hemoglobin absorption depends on its oxygenation), physiological, as opposed to anatomical maps, should also be possible.

The experiments that we present here are aimed at determining how small a localized absorbing object embedded in a highly scattering medium could be and still be detected through its effects on time-resolved photon diffusion. We also present results from an experiment to demonstrate the sensitivity to volume differences between embedded objects of the same geometrical cross section. Finally, we present time-resolved experiments to determine the path of photons introduced on the surface and detected on the same surface in the backscattering geometry. Based on these results, we present a scheme for performing a 3-D reconstruction of the absorption and scattering coefficients below the surface.

The validity of the diffusion model has been studied in both the case of a homogeneous medium[2] and in the case of a semi-infinite half plane embedded in an otherwise homogeneous medium[3]. These experiments showed that the diffusion equation was valid on the order of ten mean free paths from the source. The difficulty involved with the solutions to the diffusion equation makes comparison of experimental and theoretical results for all but the simplest systems impossible. The simple case of the semi-infinite plane, however, did show that the method of images can be applied to generate solutions to more complex problems.

Time-resolved studies can be carried out directly in the time-domain or in its Fourier transform: the frequency-domain. We have chosen to work in the frequency-domain. For measurements in highly scattering material, there are several advantages of frequency-domain methods. First, because of the finite time response of both the source and detector, a complicated deconvolution must be performed in the analysis of time-domain data. This deconvolution is simply a multiplication in the frequency-domain requiring much less data-processing time. Second, because the frequency-domain instrument does not depend on statistics of individually detected photons, its duty cycle, the time of acquisition as opposed to processing or waiting, is much higher than that of a time-domain instrument: 50 percent, as compared to 10^{-4} to 10^{-6} percent. The high duty cycle of a frequency-domain instrument allows us to implement parallel measurements without sacrificing acquisition time. Third, because in the frequency-domain the fundamental excitation is a "monochromatic," single-frequency wave, one can easily

recognize phenomena, such as diffraction, familiar from optics. One might argue that the time-domain measurement is more useful because it contains all of the harmonic frequency information, however, a single, precisely selected, frequency contains enough information for our purposes and is measured much more quickly. Thus, we focus our attention on frequency-domain studies.

2. EXPERIMENTAL RESULTS

In the frequency-domain, the fundamental excitation is a single frequency photon density wave. The wave is defined by its frequency, its average (DC) amplitude, its modulation (AC amplitude over DC amplitude) and its phase. Such a wave is generated by modulating the intensity of a light source which can be accomplished by several well-established methods. Measurement of the DC intensity, phase, and AC amplitude of the photon-density wave can be made using a frequency-domain spectrometer[4,5,6]. The fundamental components of the frequency-domain spectrometer are: an intensity-modulated light source, a heterodyning detector, and a digital acquisition system. The instrument is usually operated with modulation frequencies in the 10 to 500 MHz range and heterodyning cross-correlation frequencies in the 10 to 100 Hz range. Gated photomultiplier tubes perform the heterodyning at the detectors which produce a periodic signal at the cross-correlation frequency. The digital acquisition system is a two-channel analog-to-digital converter placed in one of the expansion slots of an IBM-compatible personal computer.

Some of our experiments were aimed at determining the detectability of a localized absorbing object through measurement of its diffraction of the photon-density wave. A complimentary set of experiments with multiple objects was done to determine how their presence contributes to the diffraction. In addition, we studied the trajectories of the diffusive photons in a model situation. These studies have lead to a better understanding of how photon diffusion might be applied to medical imaging.

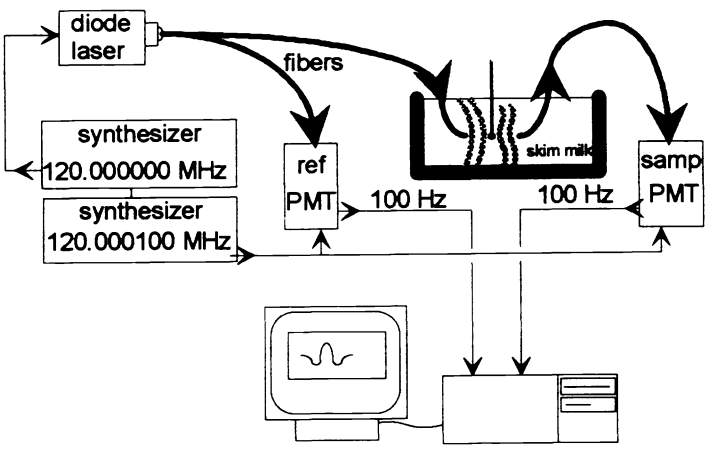

Fig. 1. Schematic of instrument.

In the experiments discussed below, a diode laser, emitting at 810 nm, coupled to a bifurcated fiber-optic-pigtail, was used as the source (see figure 1). The primary fiber carried most of the laser light to the sample. The secondary fiber carried a small fraction of the light to the reference photomultiplier tube of the instrument. The detector was a fiber bundle which picked up the light that traversed the sample and carried it to the second photomultiplier of the instrument. The laser light intensity was modulated at a radio frequency, such as 120 MHz, by varying the bias current of the diode. Sample intensity, phase difference between the sample and the reference, and normalized modulation were recorded.

The first series of experiments was aimed at determining the detectability of a small localized absorbing object. These experiments involved submerging the source and detector fibers into the scattering medium, skim milk, and spatially scanning them in a raster fashion across different objects (see figure 2). Absorbing spheres were centered between the source and detector which were separated by a distance of 5 cm. The absorbing spheres were stainless steel ball bearings painted flat black and glued to the end of clear glass pipettes. The source and detector were scanned in tandem across the spheres and the intensity, phase, and modulation of the light were measured, yielding profiles of the spheres in terms of each of these three quantities. The results of these experiments for single spheres are shown in the plots of figures 3 and 4. Results of the same experiment with more than one sphere are shown in figure 5.

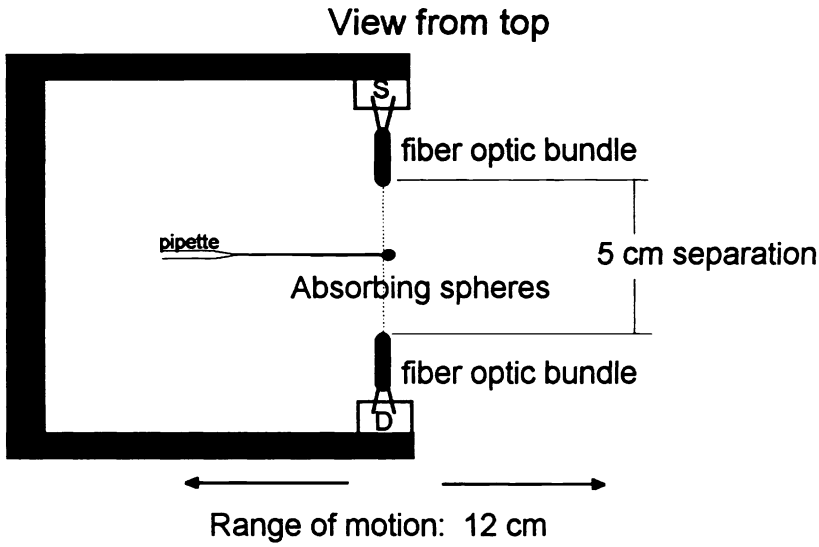

Fig. 2. Schematic of sphere scan.

To determine how well the diffusive photons samples volumes, as opposed to simple cross sections, we performed an experiment similar to the one above, using a disk instead of a sphere. The disk was positioned equidistant from both the source and the detector with its area perpendicular to the direction of the scan. The disk had the same radius as one of the spheres and was prepared in a similar fashion. Figure 6 shows the results of this experiment; note that the different diffraction patterns for a sphere and a disk are clearly distinguishable.

The results for the first series of experiments show that a small absorbing sphere has a distinct diffraction pattern (i.e., different from disk). The intensity profile is the same for all spheres in the range studied. The phase and modulation profiles, on the other hand, have distinct characteristic shapes that do not simply scale with the size of the sphere. It is also clear that very small absorbing objects (3% of the separation of the source and detector) can be seen when they are embedded in a homogeneous scattering medium. The smallest sphere, 1.6 mm diameter, was detected with a signal-to-noise ratio of about three at a modulation frequency of 90 MHz. Again, the pattern for this sphere has the characteristic shape of the other spheres, but on a much smaller scale.

There is also evidence of the volume effect one expects due to the diffusive behavior of the light. This is clear in comparing the disk and the sphere experiments. Introducing the surrounding scattering medium forces the light to sample more than simply the geometric cross section. Finally, it is clear that groups of spheres yield

different diffraction patterns than a single sphere. Reconstructing the 3-D position and size of the spheres from measured data is a problem we are presently studying.

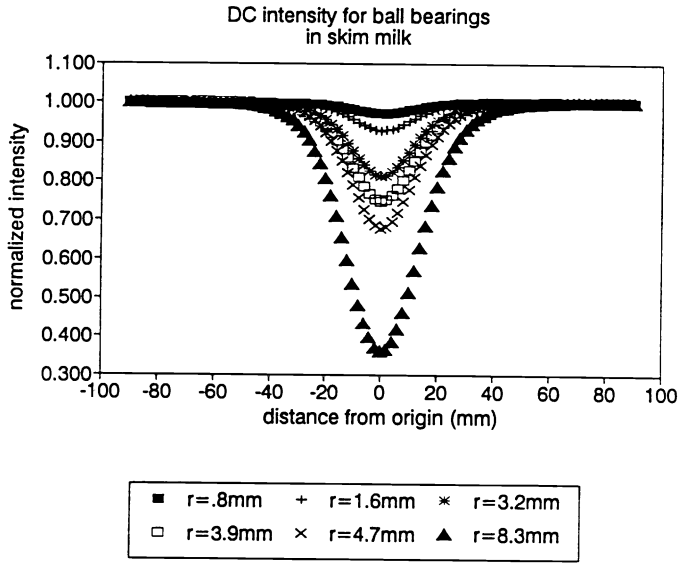

Fig. 3a. DC intensity profile of sphere experimental data.

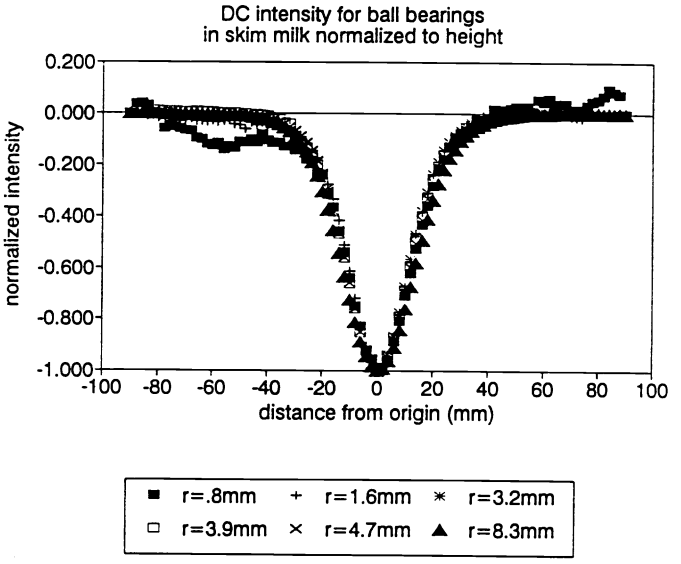

Fig. 3b. Shape of DC intensity curve is independent of sphere size.

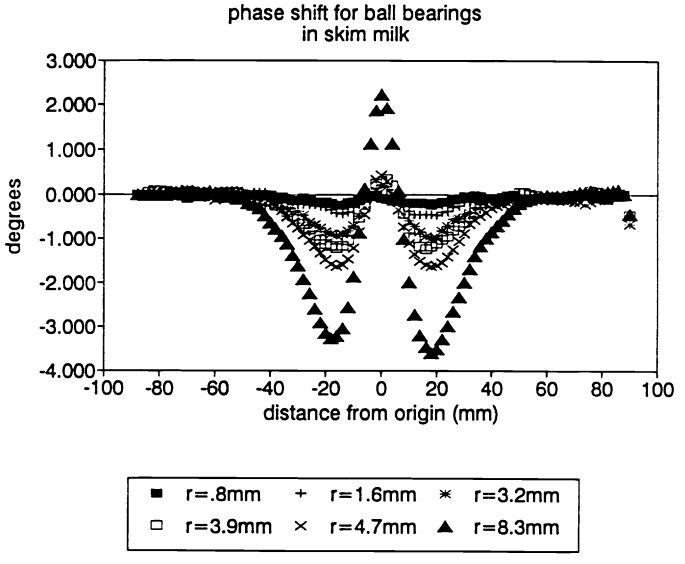

Fig. 3c. Phase profile of sphere experimental data.

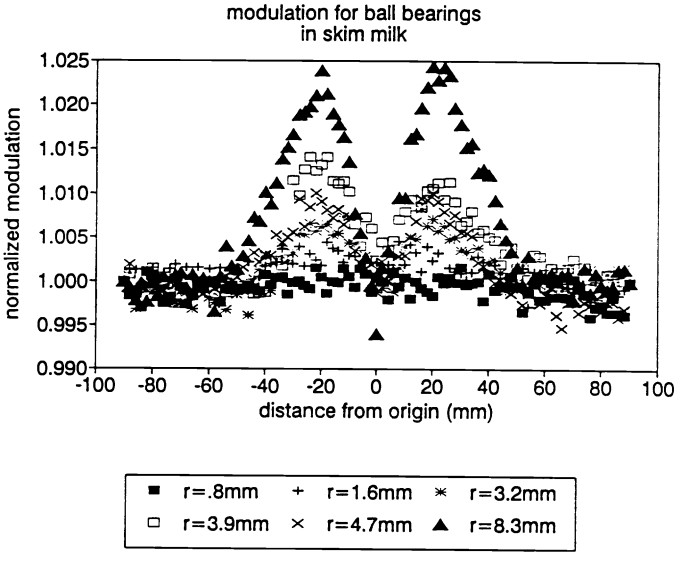

Fig. 3d. Modulation profile of sphere experimental data.

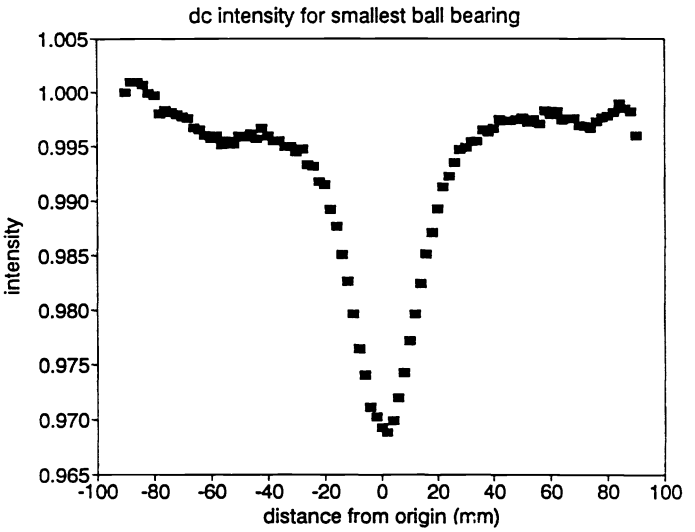

Fig. 4a. DC intensity profile of sphere experimental data with smallest sphere r = 0.8 mm.

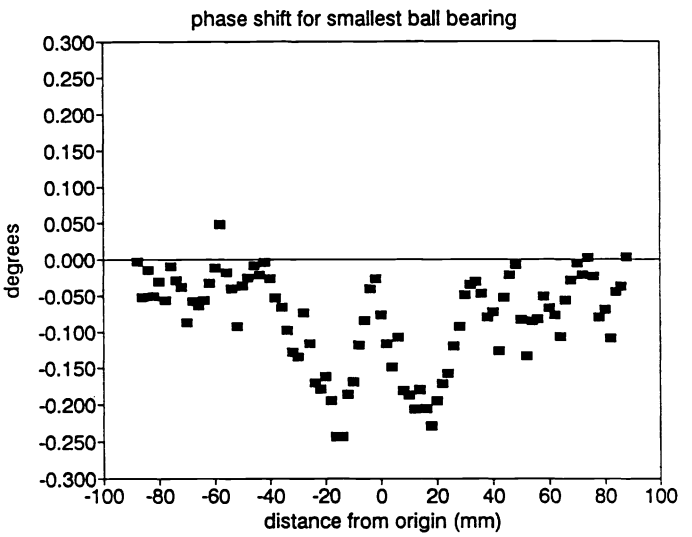

Fig. 4b. Phase profile of sphere experimental data with smallest sphere r = 0.8 mm.

A second set of experiments was done with the aim of verifying Monte Carlo simulations of photon trajectories between the source and detector on the surface of a semi-infinite scattering medium. This geometry is sometimes referred to as "backscattering geometry." The simulations predict that the photons which migrate from the source to the detector travel (on average) through a region well below the surface of the medium.

The simulated results were verified with a simple experiment. We positioned the source and detector near the surface of the milk and, with their positions fixed, we scanned a small absorbing probe in the plane perpendicular to the surface and along the line joining the source and detector (see figure 7). We measured the effect of the probe at the detector as a function of its position. The intensity signal observed at the detector was lowest when the probe was in a location that was traversed by many of the photon trajectories from the source to the detector. Using this technique, the average bundle of photon trajectories was mapped in the frequency-domain. A similar measurement in the plane perpendicular to both the surface and the line joining the source and detector was also made.

The bundle profile in terms of the intensity, phase, and modulation appears in figure 8. Single slices through the data give an alternate picture of the same system. For

Figs. 5a, b, c, d. The two close spheres are touching near the origin; the two far spheres are 5 cm apart along line equidistant from the source and detector.

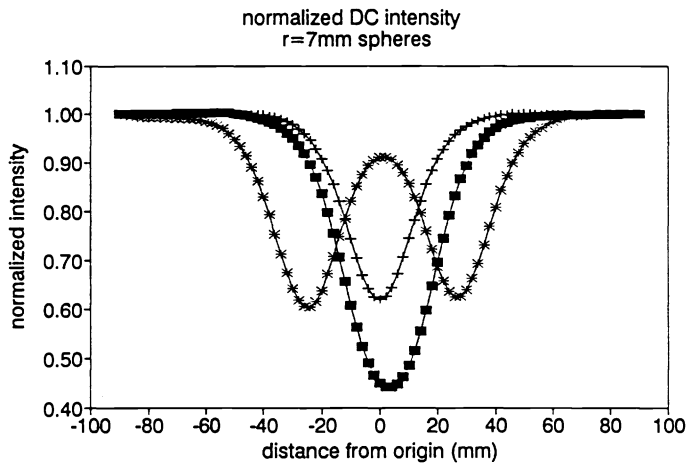

Fig. 5a. DC intensity profile of sphere experimental data with multiple spheres. -■- = 2 spheres (close), -+- = single sphere, -*- = 2 spheres (far).

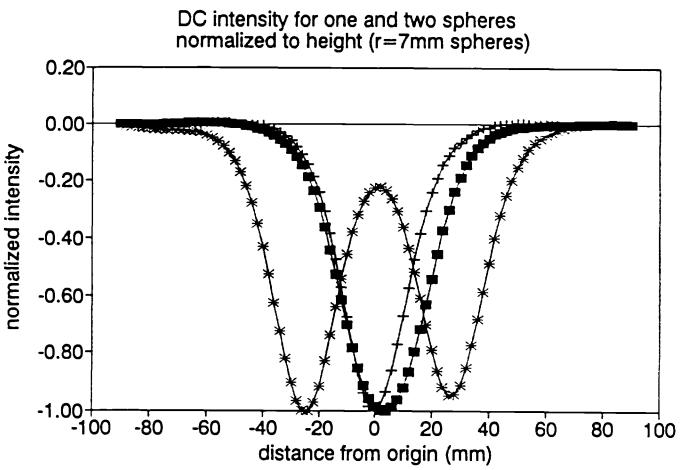

Fig. 5b. Sphere experimental data with multiple spheres showing shape of DC intensity curve is independent of sphere size . -■- = 2 spheres (close), -+- = single sphere, -*- = 2 spheres (far).

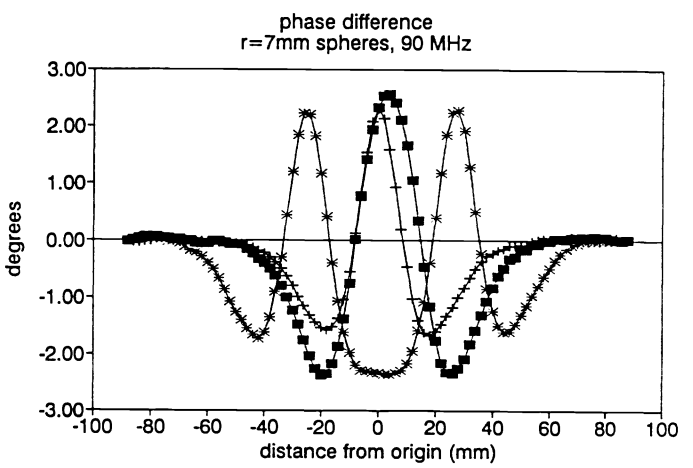

Fig. 5c. Phase profile of sphere experimental data with multiple spheres. -■- = 2 spheres (close), -+- = single sphere, -*- = 2 spheres (far).

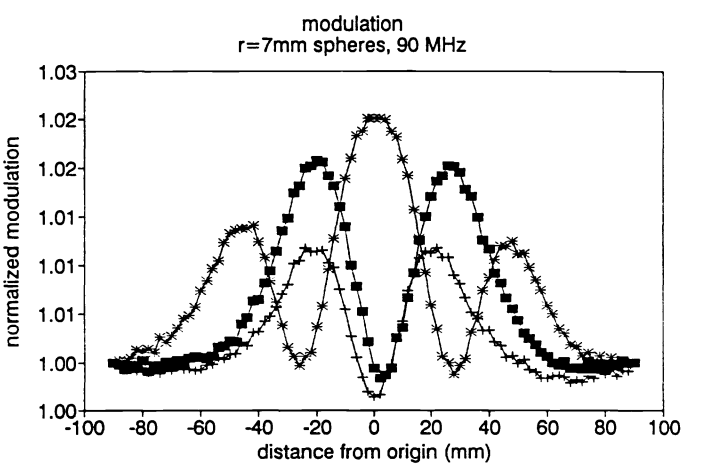

Fig. 5d. Modulation profile of sphere experimental data with multiple spheres. -■- = 2 spheres (close), -+- = single sphere, -*- = 2 spheres (far).

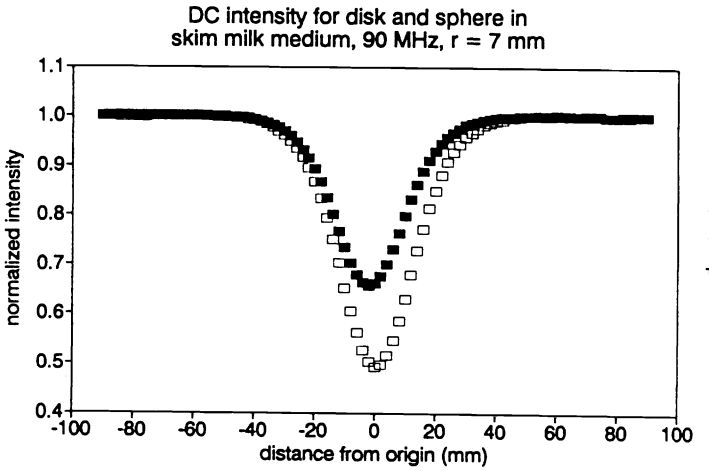

Fig. 6a. Comparison of sphere and disk data: DC intensity profile. ■ = disk, ❑ = sphere

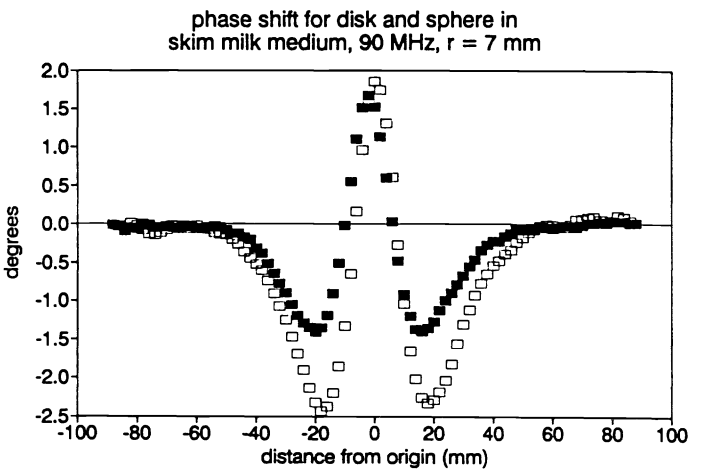

Fig. 6b. Comparison of sphere and disk data: Phase profile. ■ = disk, ❑ = sphere

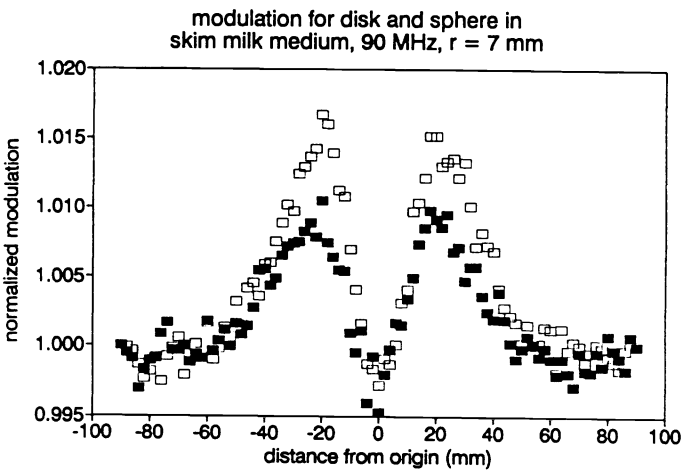

Fig. 6c. Comparison of sphere and disk data: Modulation profile. ■ = disk, ❑ = sphere

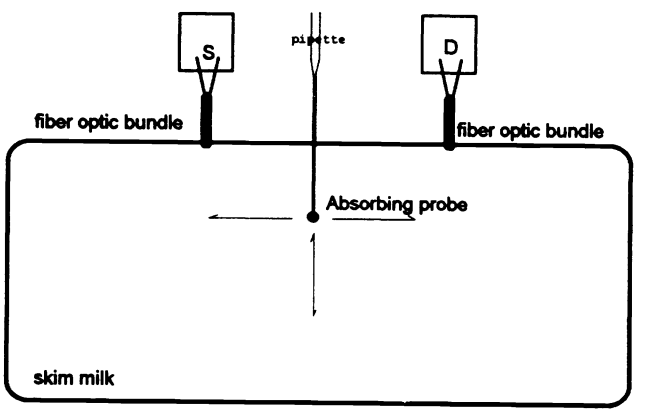

Fig. 7. Schematic of bundle experiment.

the data displayed in figure 9, the sphere was moved from above the surface to a position below the surface along a line equidistant from both the source and detector. The intensity, phase, and modulation were measured as a function of the position of the probe. To verify the effect of the size of the probe, several scans were made with different probes, all of which yielded similar results (figure 10). Of course the signal was larger and easier to measure using the larger probes.

3. DISCUSSION

The set of photon trajectories from the source to the detector form a relatively well localized bundle. The bundle of trajectories clearly travels through a region well below the surface. The maximum depth of penetration depends on the separation of the source and detector. It was consistently found to be about one-quarter of the source-detector separation distance. One would expect the penetration depth to depend on the absorption and scattering parameters but it has been shown[1] that these parameters affect the depth much less than they affect the thickness of the DC bundle of trajectories.

Based on the existence of this localized deep penetrating bundle of photon trajectories, we have devised a method of reconstruction. We will accumulate photon trajectory densities in a 3-D histogram (see figure 11), based on the standard trajectory bundle for a series of backscattering measurements on the surface. This histogram will show where the photons travel and the average absorption and scattering parameters along the path. The existence of a well-defined penetrating bundle of photon trajectories is necessary for this approach. Using the information available when time resolution is incorporated, we will be able to generate a scattering coefficient histogram and an absorption coefficient histogram. These histograms will be 3-D maps of the absorption coefficient and the scattering coefficient below the surface constructed from measurements made at the surface.

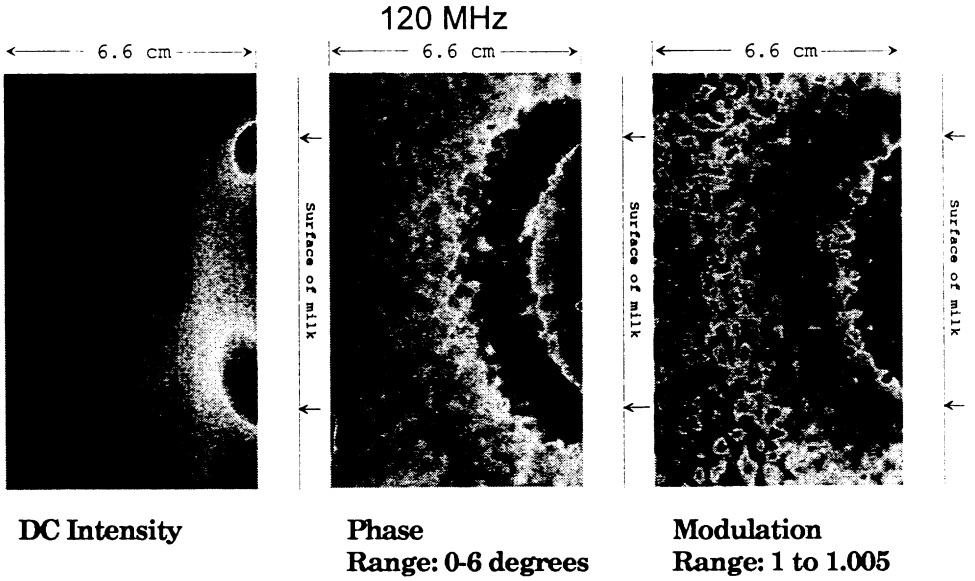

Fig. 8. Photon trajectory bundle profile.

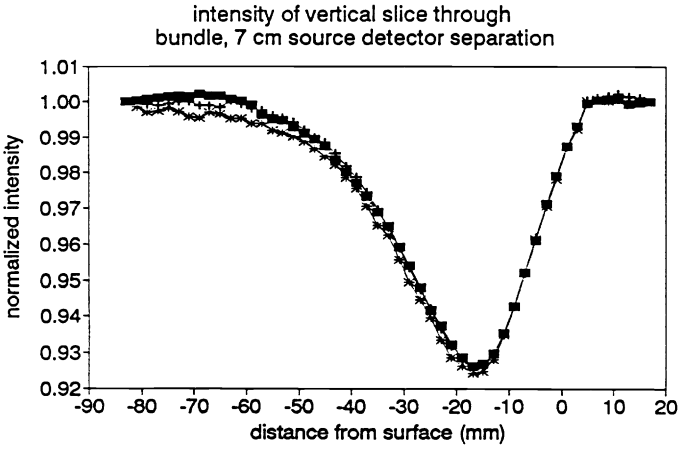

Fig. 9a. DC intensity profile of slices through bundle. —■— = 10 MHz, —+— = 90 MHz, —*— = 120 MHz.

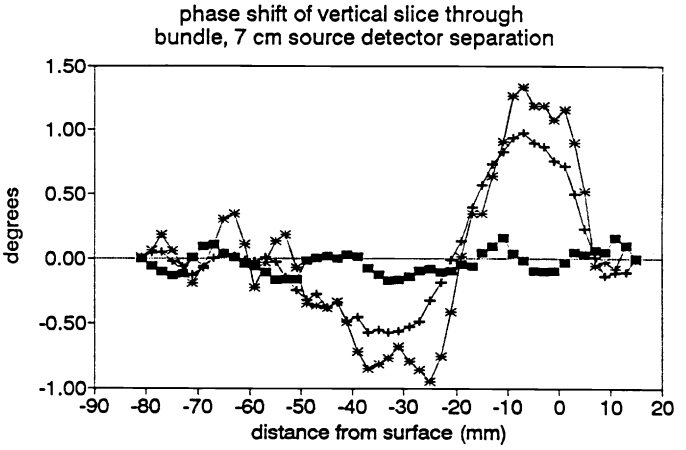

Fig. 9b. Phase profile of slices through bundle. —■— = 10 MHz, —+— = 90 MHz, —*— = 120 MHz.

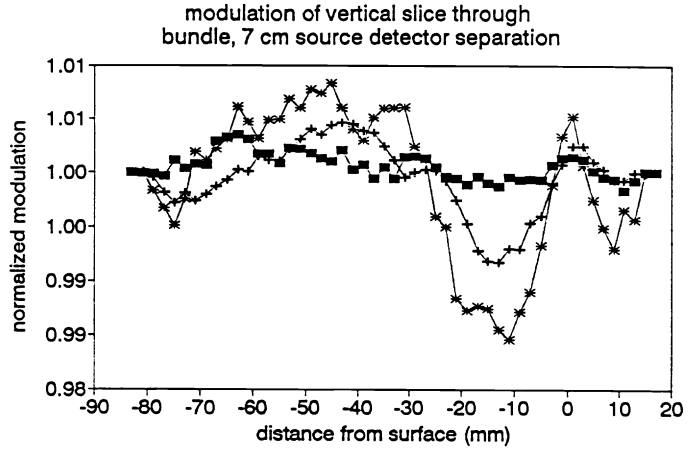

Fig. 9c. Modulation profile of slices through bundle. —■— = 10 MHz, —+— = 90 MHz, —*— = 120 MHz.

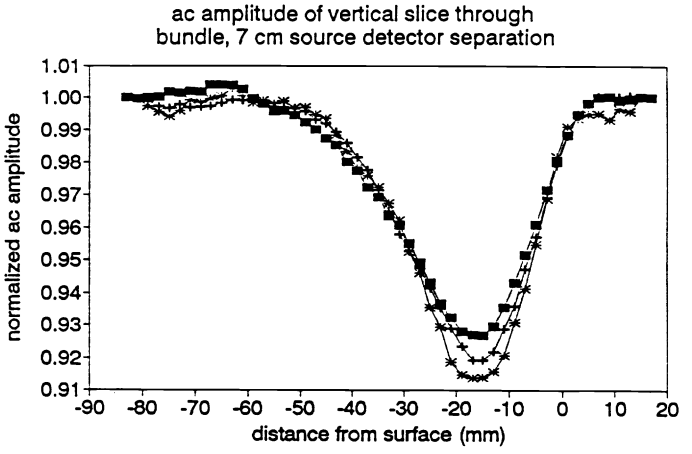

Fig. 9d. AC profile of slices through bundle. —■— = 10 MHz, —+— = 90 MHz, —*— = 120 MHz.

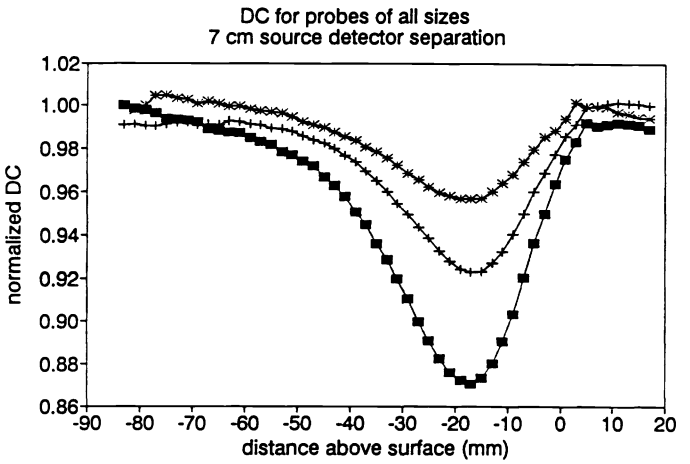

Fig. 10a. DC for probes of all sizes, 7 cm source detector separation. —■— = 6.4 mm, —+— = 4.8 mm, —*— = 3.2 mm.

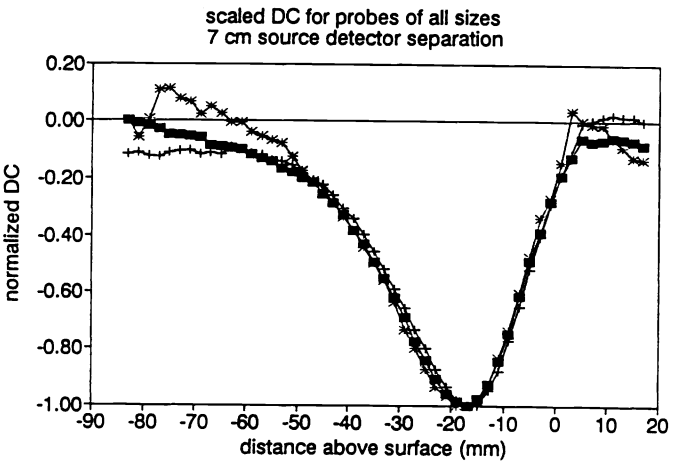

Fig. 10b. Scaled DC for probes of all sizes, 7 cm source detector separation. —■— = 6.4 mm, —+— = 4.8 mm, —*— = 3.2 mm.

4. CONCLUSIONS

Imaging of human tissues using near-infrared radiation is feasible. Frequency-domain studies of the time-resolved propagation of light in tissue are able to provide information about scattering and absorption coefficients of the tissues through which the light traveled. Our work has shown that small absorbing objects (1.6 mm diameter absorbing sphere) surrounded be highly scattering materials can be detected through their diffraction of a photon-density wave. The diffusive nature of the light propagation causes the light to sample volumes as opposed to cross sections, yielding information about the 3-D shape of the object.

We have shown that the study of the light emitted from a surface in the backscattering geometry provides information about the optical properties of the interior. The photons that migrate from the source to the detector in the backscattering geometry travel through a region well below the surface. The paths of the photons that migrate from the source to the detector in the backscattering geometry form a bundle which is relatively localized. We conclude that it is possible to study the local value of the optical parameters of the interior of the body from measurements at the surface of the body. These optical parameters can be presented in a fashion that will provide information about anatomical features or localized metabolic activity.

5. ACKNOWLEDGMENTS

These experiments, and the analyses of the data produced, were performed at the Laboratory for Fluorescence Dynamics (LFD) in the Department of Physics at the University of Illinois at Urbana-Champaign (UIUC). The LFD and this work is supported jointly by the National Institutes of Health, National Cancer Institute (CA57032) and the Division of Research Resources (RR03155) and by UIUC.

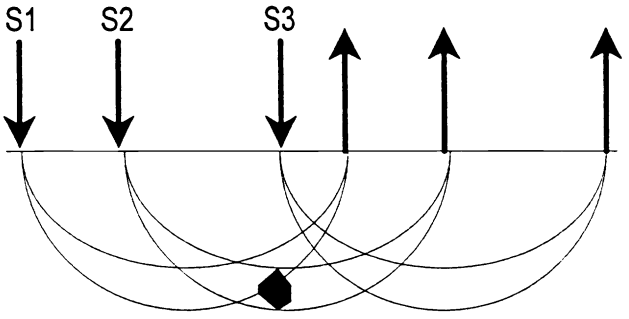

The object will affect measurement 1 (Source = S1 Detector = D1) somewhat, it will affect measurement 2 a lot and measurement 3 will be uneffected.

The model paths are plotted in a histogram with their weight corresponding to the amount the measurement at that position deviated from a standard measurement (i. e. 3 above). The regions of highest overlap correspond to the regions where objectss were detected.

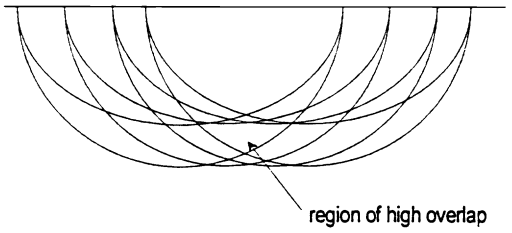

Fig. 11. Schematic of reconstruction.

6. REFERENCES

1. Cui, W., C. Kumar, B. Chance, 1991. Experimental study of migration depth for the photons measured at sample surface, *SPIE Vol. 1431, Time-Resolved Spectroscopy and Imaging of Tissues*, pp. 180-191.

2. Fishkin, J. B., Gratton, E., 1991. Diffusion of intensity modulated near-infrared light in turbid media, *SPIE Vol. 1431, Time-Resolved Spectroscopy and Imaging of Tissue*, pp. 122-135.

3. Fishkin, J. B., Gratton, E., 1992. Propagation of photon density waves in strongly scattering media containing an absorbing "semi-infinite" plane bounded by a straight edge, *J. Optical Soc. of America*, in press.

4. Gratton, W., M. Limkeman, 1983. A continuously variable frequency cross-correlation phase fluorometer with picosecond resolution. *Biophys. J., 44*, 315.

5. Alcala, J. R., E. Gratton, and D. M. Jameson, 1985. A multifrequency phase fluorometer using the harmonic content of a mode-locked laser, *Analytical Instrumentation, 14*, 225.

6. Feddersen, B. A., D. W. Piston and E. Gratton, 1989. Digital parallel acquisition in frequency domain fluorometry, *Rev. Sci. Inst., 60*, 2929.